Available online at www.sciencedirect.com
ScienceDirect
International Journal of Pharmaceutics 335 (2007) 54–62
INTERNATIONAL JOURNAL OF PHARMACEUTICS
www.elsevier.com/locate/ijpharm

Optimization and scale-up of a fluid bed tangential spray rotogranulation process

J. Bouffard [a], H. Dumont [b,*], F. Bertrand [a], R. Legros [a]

[a] *Department of Chemical Engineering, École Polytechnique de Montréal, P.O. Box 6079, Stn. Centre-Ville, Que. H3C 3A7, Canada*
[b] *Pharmaceutical Research and Development, Merck Frosst Canada Ltd., Kirkland, Que. H9H 3L1, Canada*

Received 12 July 2006; accepted 27 October 2006
Available online 12 November 2006

Abstract

The production of pellets in the pharmaceutical industry generally involves multi-step processing: (1) mixing, (2) wet granulation, (3) spheronization and (4) drying. While extrusion-spheronization processes have been popular because of their simplicity, fluid-bed rotogranulation (FBRG) is now being considered as an alternative, since it offers the advantages of combining the different steps into one processing unit, thus reducing processing time and material handling. This work aimed at the development of a FBRG process for the production of pellets in a 4.5-l Glatt GCPG1 tangential spray rotoprocessor and its optimization using factorial design. The factors considered were: (1) rotor disc velocity, (2) gap air pressure, (3) air flow rate, (4) binder spray rate and (5) atomization pressure. The pellets were characterized for their physical properties by measuring size distribution, roundness and flow properties. The results indicated that: pellet mean particle size is negatively affected by air flow rate and rotor plate speed, while binder spray rate has a positive effect on size; pellet flow properties are enhanced by operating with increased air flow rate and worsened with increased binder spray rate. Multiple regression analysis enabled the identification of an optimal operating window for production of acceptable pellets. Scale-up of these operating conditions was tested in a 30-l Glatt GPCG15 FBRG.

Keywords: Rotogranulator; Granulation; Process optimization; Scale-up; Pellets

1. Introduction

With fluid bed rotogranulation (FBRG), spherical and dense pellets are obtained in a hermetic single pot processor, as opposed to the multi-step extrusion-spheronization technique. The overall manufacturing time required is generally shorter and material handling considerably reduced. However, the product final properties are strongly affected by FBRG process parameters (Vertommen and Kinget, 1997; Gu et al., 2004), thus demanding in-depth characterization of the operation window in order to develop a robust and scalable process. It is well known that product final properties and process yield are controlled by mixing intensity and the water content present in the formulation (Ghebre-Sellasie and Knoch, 2002). Fluidizing air flow rate, gap space between the rotor disc and the unit wall, bed mass, disc velocity and its surface morphology are the main parameters affecting mixing, while binder solution flow rate, atomization pressure and inlet air temperature affect the fluid bed moisture content. Operating variables and material properties which influence the final product have been studied for the FBRG process (Vertommen and Kinget, 1997; Rashid et al., 1999; Kristensen et al., 2000; Holm et al., 1996).

1.1. Disc velocity

A helicoidal flow pattern is a characteristic of FBRG, which is essential for an efficient spheronization of the agglomerates and an adequate liquid distribution on the bed particles. At low disc velocity, this motion profile disappears and the excessive agglomeration that follows can induce the formation of lumps and material deposition on the processor walls. At high disc velocity, particle–particle and particle–wall contacts increase as the bed turn-over also increases. It creates a chaotic flow pattern in the bed and yields to increased particle breakage, which can compromise granulation and dosage uniformity of a pharmaceutical product (Ghebre-Sellasie and Knoch, 2002).

Korakianiti et al. (2000) mentioned that disc velocity can affect differently the final product depending on the formula-

* Corresponding author. Tel.: +1 514 428 2859; fax: +1 514 428 4945.
E-mail address: hubert_dumont@merck.com (H. Dumont).

0378-5173/$ – see front matter © 2006 Elsevier B.V. All rights reserved.
doi:10.1016/j.ijpharm.2006.11.022

tion and the manufacturing method used for FBRG processes. Higher disc velocity can cause larger (Vertommen and Kinget, 1997; Rashid et al., 1999; Kristensen et al., 2000; Vilhelmsem et al., 2004; Pišek et al., 2000; Wan et al., 1993; Rashid, 2001; Liew et al., 2000), unchanged (Holm et al., 1996) and smaller (Korakianiti et al., 2000) granules. It can narrow the particle size distribution (Korakianiti et al., 2000; Vilhelmsem et al., 2004; Pišek et al., 2000; Liew et al., 2000) or widen it (Vertommen and Kinget, 1997). It can also improve the granule roundness (Pišek et al., 2000, 2001; Wan et al., 1993; Liew et al., 2000) or worsen it (Rashid et al., 1999; Pišek et al., 2000; Rashid, 2001). It is clear that disc velocity effects must be better understood, since improper selection of this parameter can lead to undesirable results.

1.2. Air flow rate and gap air pressure

A reduction of the air flow rate or gap air pressure decreases the helicoidal flow pattern in the bed (Ghebre-Sellasie and Knoch, 2002). To obtain an efficient process, the air gap must be small enough to avoid material falling below the disc, but also to minimize powder build-up in the filters due to elutriation. Wan et al. (1994) indicate that the particle size is reduced when the gap air pressure is increased. This is explained by higher shearing forces induced by an intensified helicoidal flow pattern. They also mention that an increase in air gap pressure can induce a higher moisture loss, which contributes to a reduction of the particle size.

1.3. Bed moisture content

Bed moisture content is a critical property in rotogranulation and it has to be evaluated with caution. There are three main factors that affect the bed moisture content: air flow rate, air temperature and binder flow rate. A low bed moisture content leads to coarse granules that are very porous, since they grow by a crushing and layering mechanism. The final granules are generally weak and deformable (Iveson et al., 2001). When the binder flow rate increases, the granule growth is promoted. This can be explained by a greater binder availability at the granule surface, which favors coalescence. At higher binder content, consolidation is also favored and the final granules are generally stronger and deform less easily (Iveson et al., 2001). They are also generally less porous than in the case of granulation at lower moisture content.

1.4. Scale-up

Different methods can be used to extrapolate an industrial process: dimensionless analysis, mathematical models and simulation. In general, scale-up criteria are obtained by a trial and error method combined with geometric similarity principles that involve dimensionless analysis (Chukwumezie et al., 1994).

1.4.1. Disc velocity

For rotor granulators, two criteria are often used to determine disc velocity during scale-up: (1) constant Froude number or (2) constant disc peripheral velocity (Perry and Green, 1997) which are presented in Eqs. (1) and (2), respectively. In these equations, d, m and N are the disc diameter in meter, the bed mass in kilogram and the disc rotational velocity in rpm, respectively. The subscripts s and l mean the small and large-scale units. The Froude number has been modified according to Horsthuis and Laarhoven (1993) and considers that centrifugal force is directly proportional to the weight of the powder blend and the square of the rotational speed and inversely related to the plate radius.

$$N_\mathrm{l} = \sqrt{\frac{m_\mathrm{s}}{m_\mathrm{l}}\frac{d_\mathrm{l}}{d_\mathrm{s}}N_\mathrm{s}^2} \tag{1}$$

$$N_\mathrm{l} = \frac{d_\mathrm{s}}{d_\mathrm{l}}N_\mathrm{s} \tag{2}$$

1.4.2. Binder flow rate

To obtain a product that is similar at small and large scales, the bed moisture content has to be monitored correctly. Binder flow rate and air flow rate jointly affect the bed moisture content and cannot be scaled separately.

The bed mass can also affect the bed moisture content. It must be conveniently scaled from the small to the large-scale units. If it is not the case, a correction factor has to be inserted in the air flow rate scale-up expression. The relation is valid only for the systems that are perfectly mixed, which implies that binder solution is uniformly distributed in the fluid bed. Knowing the working volume and the bed mass used at small-scale, the correction factor is:

$$f = \frac{V_\mathrm{l} m_\mathrm{s}}{V_\mathrm{s} m_\mathrm{l}} \tag{3}$$

where V is the working volume of the equipment in m^3.

1.4.3. Air flow rate

In wet granulation systems that use fluid beds, the exhaust air and product temperature reach an equilibrium. This equilibrium state is directly associated to an adiabatic saturation of the air as it passes through the bed of wet particles. This means that water injected in the bed with the binder solution (xB_l) is completely removed by evaporation ($A_\mathrm{v}\rho_\mathrm{v}$). The drying air capacity (D_c) expressed as the mass of water added per mass of dry air can be easily determined on a psychometric chart as a function of inlet air conditions. The mass balance over the fluid bed at equilibrium is given by:

$$A_\mathrm{l}\rho_\mathrm{a} = A_\mathrm{v}\rho_\mathrm{v} + A_\mathrm{da}\rho_\mathrm{a} = xB_\mathrm{l} + A_\mathrm{da}\rho_\mathrm{a} \tag{4}$$

where A, B, x and ρ are the air flow rate in m^3/s, the binder flow rate in kg/s, the mass fraction of water in liquid binder and the density in kg/m^3, respectively. The subscripts a, da and v mean in the same order the wet air, dry air and water vapor.

And the expression for the drying air capacity (kg water/kg dry air) reads as:

$$D_\mathrm{c} = \frac{xB_\mathrm{l}}{A_\mathrm{da}\rho_\mathrm{a}} \tag{5}$$

Considering that D_c should be set to keep the same drying capacity for the scale-up, the following relation can be obtained

by combining Eqs. (4) and (5):

$$A_1 = \frac{xB_l(1 + D_c)}{\rho_a D_c} \quad (6)$$

This relation can be used to adjust the air flow rate versus the binder liquid flow rate to keep D_c constant. The introduction of the correction factor (f) in Eq. (6) allows to predict more accurately the air flow rate as a function of bed mass variation:

$$A_1 = \frac{xB_l(1 + D_c)}{\rho_a D_c} f \quad (7)$$

The relations seen earlier are valid at steady state and it is essential to verify that the rotogranulations with the GPCG1 reaches this state to be scalable. The air outlet temperature can be used to detect when the steady state is reached. It is the case when this temperature becomes constant, at a value corresponding to the adiabatic saturation state.

The optimization and scale-up are aspects that have not been covered extensively. This study presents the optimization of an operating window for a small-scale FBRG system using a factorial design together with the development of scale-up criteria.

2. Materials and methods

2.1. Process parameters

There are two phenomena that mainly affect the rotogranulation: the solid flow pattern, that influences the particle collision velocity and frequency, and the moisture content that plays a role in the particle cohesion through capillary forces and breakage mechanisms. The process parameters that are studied in this work are presented in Table 1 along with their respective operating limits. These parameters are relevant to the granulation process, as discussed earlier. The low inlet air temperature used (30 °C) allows to operate in a more sensitive zone of the drying air capacity which promotes net process responses to inlet air temperature and moisture content adjustments thus providing more flexibility on scale-up. It also mimics processing conditions encountered with heat sensitive drugs.

2.2. Equipment and formulation

Instrumented tangential spray rotoprocessors GPCG1 and GPCG15 (Glatt; Ramsey N.J.) were used for this study. The statistical analysis and process optimization were carried out with the GPCG1, and the extrapolation study was achieved using the GPCG15.

Table 1
Process parameters and operating limits range

Parameters	Operation limits
Disc velocity (a)	400–1000 rpm
Air gap pressure (b)	1.5–2.0 kPa
Air flow rate (c)	150–180 m^3/h
Binder flow rate (d)	12–15 g/min
Atomization pressure (e)	140–210 kPa

Inlet air temperature, 30 °C; disc surface type, smooth.

Table 2
Excipient proportions in final product for GPCG1 and GPCG15

Excipients	Proportion (wt.%)
Acetaminophen 98.0–101.0% (Sigma–Aldrich Inc.)	25
MCC PH-101 (FMC Biopolymer Corp.)	50
Lactose monohydrate (Foremost Farm USA)	17
Hydroxypropyl cellulose LF (Hercules Inc.)	8

Table 2 presents the formulation used for this study. The bed mass for the small-scale experimentation started at 460 g. Binder liquid contained 8 wt.% of HPC and the total solution mass sprayed was 500 g. The dry powder mass at the end of the process was 500 g.

At large-scale, the bed mass started at 9.2 kg. The binder liquid contains the same HPC concentration but the total solution mass sprayed was 10 kg to reach a dry powder mass of 10 kg. Two formulations were used at large-scale. Table 3 presents the placebo formulations in which acetaminophen has been replaced by MCC and lactose. The trial formulations were using the excipients mentioned in Table 2.

2.3. Characterization of final product properties

The properties evaluated for the granules produced during an experiment were: (1) mean size and particle size distribution, (2) bulk and tapped density to calculate the Carr's index, (3) granule roundness and (4) acetaminophen dosage. Mean size and particle size distribution were measured by sieve analysis. The bulk and tapped densities were measured from a Vankel tap density apparatus. Image analysis was used to evaluate the pellet roundness from the following expression:

$$\text{roundness} = \frac{P_t}{P_r} \quad (8)$$

where P_t is the theoretical perimeter of a perfectly spherical granule of equal area as the real one and P_r is the real granule perimeter.

Acetaminophen content was assayed by UV spectroscopy based on a USP dissolution method for acetaminophen tablets and reported as the percentage of the theoretical label claim. For the experimental design, a composite sample of each experiment was analyzed. For the optimized and scale-up experiments, samples from 10 sampling locations were analyzed to establish the drug content uniformity of the material.

2.4. Experimental design

Fig. 1 presents the operation procedure for all the experiments. The process parameter values for the drying step were set to limit breakage of the granules. A 2^{5-1} fractional facto-

Table 3
Excipient proportions in placebo used for GPCG15

Excipients	Proportion (wt.%)
MCC PH-101 (FMC Biopolymer Corp.)	69
Lactose monohydrate (Foremost Farm USA)	23
Hydroxypropyl cellulose LF (Hercules Inc.)	8

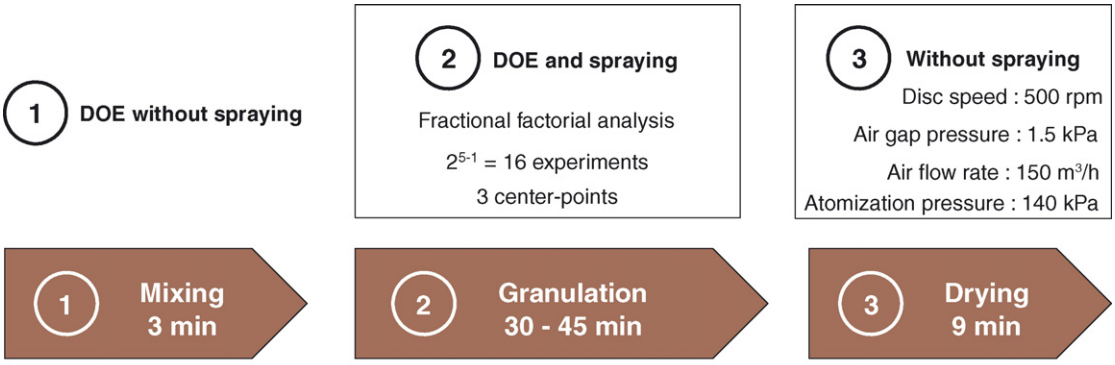

Fig. 1. Experimental procedure.

rial design was prepared to statistically analyze the final product properties mentioned above. Sixteen experiments were carried out, which correspond to two levels for the five process parameters (see Table 4) with three center points. SEM pictures were also taken to compare the different results qualitatively.

The statistical analysis was performed using the JMP software (Version 5.0.1, SAS institute). A linear regression was performed on the data for each characteristic as a function of the five process parameters and their interactions. Optimization of the process was carried out using the following criteria:

(1) Particle size distribution must have a R.S.D. < 1.4 (Edmundson, 1967)
(2) Mean size ($\bar{\mu}$) must be larger than 300 μm and smaller than 600 μm.
(3) Powder must possess a Carr's index $< 18\%$ (Wells and Aulton, 1988).
(4) Roundness factor must be superior to 0.75.
(5) Acetaminophen drug content must assay between 95% and 105% of the theoretical label claim, i.e 25% or 250 mg/g.

An optimized window of the five process parameters were determined for the small-scale unit (GPCG1). This window of operating parameters was then scaled up to the larger unit (GPCG15) using the criteria described in Section 1.4. For the needs of this study, the binder flow rate was set at 60 g/min to reduce the operation time below 3 h.

3. Results and discussion

3.1. Characterization of final product properties

Table 4 presents the results from the characterization of the 19 experiments. This information was statistically analyzed to obtain the linear regressions used for the optimization process.

3.2. Statistical analysis

Tables 5–7 present the normalized results from the statistical analysis obtained using the software JMP. The linear regression yields the coefficients multiplying each of the five process pa-

Table 4
Characterization results

Experiment no.	Parameter adjustments	$\bar{\mu}$ (μm)	R.S.D. (%)	Carr's index (%)	True density (g/ml)	Roundness	Drug content assay (%LC)
1	abcdE	383	1.32	18.89	1.55	0.75	100.0
2	Abcde	407	1.44	18.84	1.49	0.73	99.9
3	aBcde	360	1.33	20.43	1.50	0.73	100.8
4	ABcdE	365	1.42	21.51	1.51	0.72	99.0
5	abCdE	381	1.38	22.63	1.55	0.73	101.8
6	AbCdE	350	1.75	21.86	1.47	0.68	98.3
7	aBCdE	318	1.66	26.15	1.54	0.75	98.7
8	ABCde	260	1.60	29.62	1.52	0.65	97.6
9	abcDe	570	1.64	17.64	1.51	0.74	100.6
10	AbcDE	575	1.73	14.16	1.50	0.77	98.2
11	aBcDE	646	1.40	12.07	1.50	0.79	100.2
12	ABcDe	402	1.42	17.34	1.52	0.82	100.8
13	abCDE	385	1.33	21.26	1.53	0.82	100.4
14	AbCDe	353	1.41	20.22	1.55	0.81	101.6
15	aBDCe	522	1.57	16.79	1.53	0.78	103.3
16	ABCDE	432	1.41	22.10	1.51	0.80	97.4
17	00000	373	1.32	17.99	1.60	0.78	96.0
18	00000	380	1.33	19.90	1.53	0.81	97.4
19	00000	397	1.35	15.91	1.58	0.78	95.2

Large subscripts (ABCDE) represent the upper limit of operation and small subscripts (abcde) the lower limit. Aa, disc velocity; Bb, air gap pressure; Cc, air flow rate; Dd, binder flow rate; Ee, atomization pressure.

Table 5
Results for mean size and particle size distribution

Parameters and interactions	$\bar{\mu}$ ($r^2 = 0.98$)		R.S.D. ($r^2 = 0.84$)	
	Coefficient	*P*-value	Coefficient	*P*-value
Constant	413.6	< 0.01	1.46	< 0.01
Disc velocity (*a*)	-26.3	0.05	0.03	0.41
Air gap pressure (*b*)	-6.2	0.53	-0.01	0.76
Air flow rate (*c*)	-44.2	0.01	0.03	0.52
Binder flow rate (*d*)	66.3	< 0.01	0.00	0.99
Atomization pressure (*e*)	12.4	0.25	0.01	0.71
(*a*) × (*b*)	-22.1	0.08	-0.05	0.27
(*a*) × (*c*)	-0.1	0.99	-0.01	0.88
(*a*) × (*d*)	-18.8	0.12	-0.03	0.45
(*a*) × (*e*)	25.1	0.06	0.04	0.34
(*b*) × (*c*)	14.1	0.20	0.06	0.20
(*b*) × (*d*)	21.1	0.09	-0.03	0.51
(*b*) × (*e*)	14.7	0.19	-0.02	0.65
(*c*) × (*d*)	-18.4	0.12	-0.08	0.10
(*c*) × (*e*)	-16.3	0.16	0.01	0.81
(*d*) × (*e*)	11.4	0.28	-0.04	0.39

Table 7
Results for drug content assay

Parameters and interactions	Drug content assay (%LC) ($r^2 = 0.52$)	
	Coefficient	*P*-value
Constant	99.33	< 0.01
Disc velocity (*a*)	-0.81	0.42
Air gap pressure (*b*)	-0.19	0.84
Air flow rate (*c*)	-0.03	0.98
Binder flow rate (*d*)	0.40	0.68
Atomization pressure (*e*)	-0.89	0.39
(*a*) × (*b*)	-0.21	0.82
(*a*) × (*c*)	-0.35	0.72
(*a*) × (*d*)	< 0.01	1.00
(*a*) × (*e*)	0.01	0.99
(*a*) × (*c*)	-0.45	0.64
(*b*) × (*d*)	0.30	0.76
(*b*) × (*e*)	-0.01	0.99
(*c*) × (*d*)	0.39	0.69
(*c*) × (*e*)	-0.30	0.76
(*d*) × (*e*)	-0.38	0.70

rameters or their interactions for each final product property. The *P*-value, which is the significance indicator, is also calculated and presented in these tables.

As can be seen, the granule mean size decreases when either the disc velocity ($P = 0.05$), or the air flow rate ($P = 0.01$) are increased, or when the liquid binder flow rate is decreased ($P < 0.01$). The Carr's index, which is an indicator for the powder flowability, improves with an increase of liquid binder flow rate ($P = 0.03$) or a decrease of air flow rate ($P = 0.03$). The granular roundness is accentuated with a higher liquid binder flow rate ($P = 0.03$). Concerning the particle size distribution and drug content assay, they are not significantly affected by the process parameters as they remain relatively constant and within acceptable limits.

For all properties, except for particle size distribution and drug content assay, two process parameters are dominant: air flow rate and liquid binder flow rate. This confirms that the water content of granules is a critical factor that affects the particle and powder bed properties. Fig. 2 compares the morphology of granules with respect to the water addition rate during the granulation for different process operating conditions. These pictures clearly demonstrate the effect of both air flow rate and binder flow rate, as evidenced by the statistical analysis.

Literature suggests that, contrary to top spray granulation, rotogranulation process is not affected significantly by the droplet size distribution. The shear created by the disc minimizes the impact of the droplet size on the granule final properties. It is suspected that the liquid bridges alone are not strong enough to retain the particles in the newly formed agglomerates when they contact the granulator disc (Holm et al., 1983; Ax et al., 2006). The coalescence rather results from the particle collisions that deform the granules and promote larger contact area to bind them (Iveson et al., 2001). This mechanism of granule formation is enhanced by moisture content and the droplet size distribution has very little effect.

Table 6
Results for Carr's index and roundness

Parameters and interactions	Carr's index ($r^2 = 0.93$)		Roundness ($r^2 = 0.91$)	
	Coefficient	*P*-value	Coefficient	*P*-value
Constant	19.75	< 0.01	0.761	< 0.01
Disc velocity (*a*)	0.61	0.41	-0.006	0.51
Air gap pressure (*b*)	0.66	0.38	0.002	0.84
Air flow rate (*c*)	2.48	0.03	-0.002	0.84
Binder flow rate (*d*)	-2.40	0.03	0.036	0.03
Atomization pressure (*e*)	-0.34	0.63	0.005	0.59
(*a*) × (*b*)	1.28	0.14	-0.002	0.86
(*a*) × (*c*)	0.26	0.71	-0.010	0.34
(*a*) × (*d*)	0.15	0.84	0.015	0.18
(*a*) × (*e*)	-0.45	0.53	-0.011	0.31
(*a*) × (*c*)	0.43	0.55	-0.008	0.42
(*b*) × (*d*)	-1.28	0.14	0.007	0.51
(*b*) × (*e*)	0.05	0.94	0.004	0.67
(*c*) × (*d*)	-0.09	0.90	0.014	0.22
(*c*) × (*e*)	0.61	0.41	0.004	0.70
(*d*) × (*e*)	0.04	0.95	-0.003	0.79

3.3. Process optimization

Insertion of the optimization criteria, described earlier in Section 2.4, into the predictive model obtained with the JMP software makes it possible to obtain the optimal process parameter values for a given set of final product properties. An experiment was carried out using this set of optimal process parameter conditions. Table 8 presents the measured final product properties of the experiments compared with the statistical model predictions. The drug content assay reveals that the optimized product is within the desired criteria.

The maximum deviation observed is 6%, which indicates that the model is efficient for predicting the granular properties as a function of the process parameters. Also, all characteristic values comply with the desired product criteria. Fig. 3 shows the granules obtained from the optimal run with GPCG1.

Table 8
Rotogranulation process optimization and statistical model validation

Process parameters: $a = 730$ rpm; $b = 2$ kPa; $c = 148.8\ m^3/h$; $d = 13.65$ g/min; $e = 151.7$ kPa			
	Predicted properties	Experimental properties	Deviation (%)
$\bar{\mu}$ (μm)	416	442	6
R.S.D. (%)	1.38	1.40	1
Carr's index (%)	18	17	6
Roundness	0.77	0.81	6
Drug content uniformity (%LC)		102.2% (R.S.D. = 1.5%)	

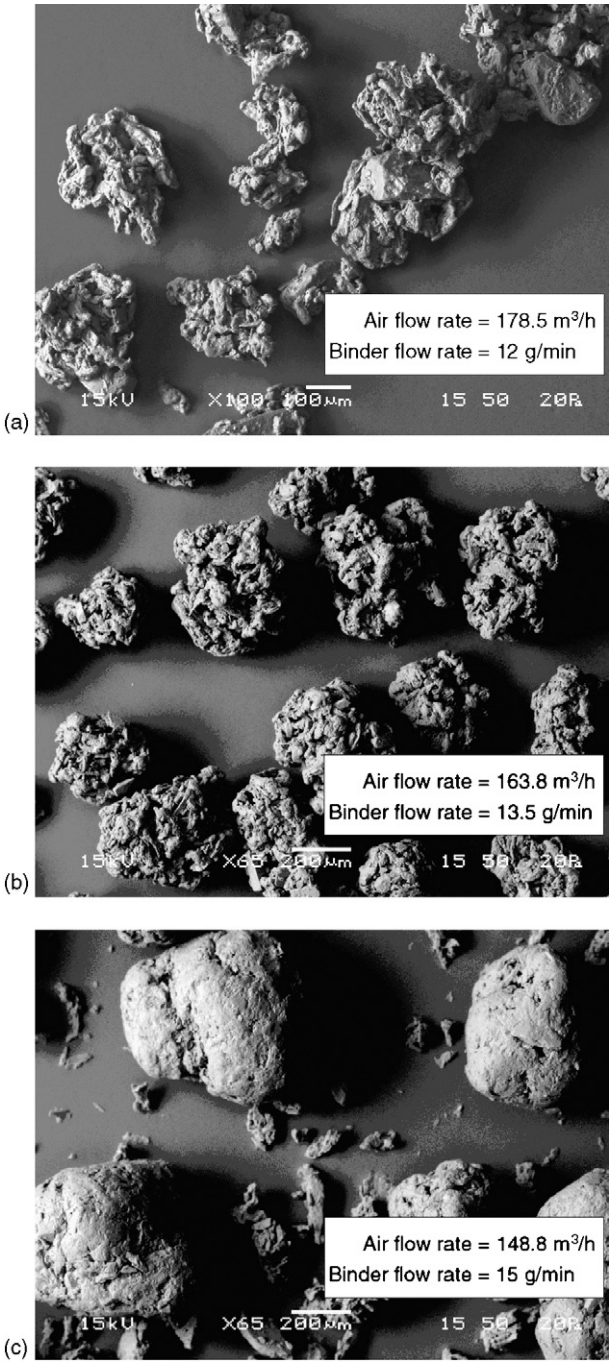

Fig. 2. Granular morphology for different water addition rates: (a) experiment 8, (b) experiment 18 and (c) experiment 11.

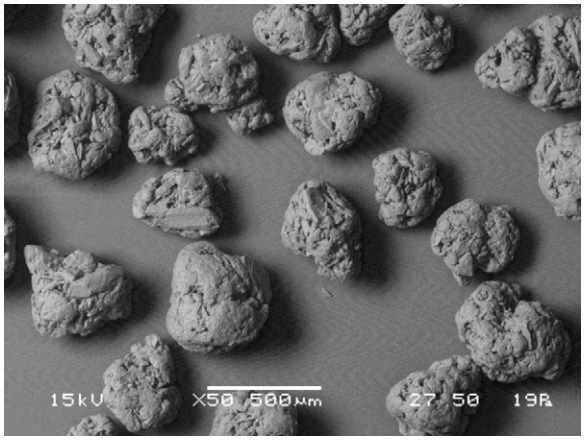

Fig. 3. GPCG1 optimal run.

3.4. Process scale-up

As mentioned in Section 1.4.3, it was important to verify that all experiments reached steady-state conditions to ensure the validity of the final product properties. For example, Fig. 4 presents the outlet temperature for the 19 experiments as a function of time. It can be readily seen that the equilibrium is maintained for more than half the total granulation time.

Because large quantities of material are necessary for large-scale granulation experiments, placebo tests were first prepared to verify which scale-up method should be used for disc velocity and air flow rate. Table 9 presents the two sets of operating parameters used for the large-scale equipment with the placebo products. In particular, binder flow rate was fixed at 60 g/min

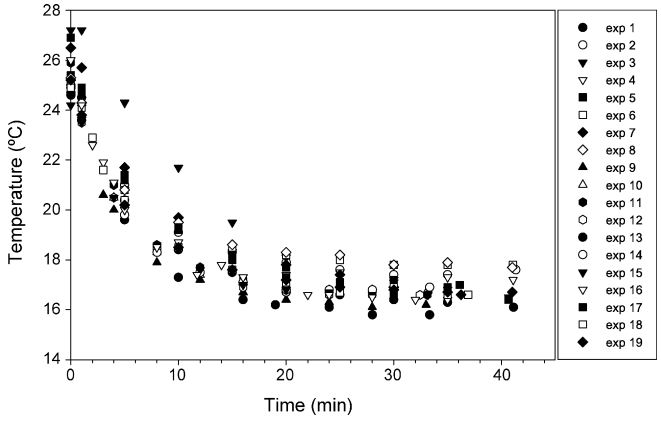

Fig. 4. Temperature evolution for the 19 rotogranulations.

Table 9
Placebo rotogranulation scale-up parameters

	GPCG15 criteria 1	GPCG15 criteria 2
Disc speed (rpm)	200	440
Air gap pressure (kPa)	2	2
Air flow rate (m^3/h)	475.7	148.7
Binder flow rate (g/min)	60	60
Atomization pressure (kPa)	151.7	151.7

Table 10
Acetaminophen rotogranulation scale-up parameters

	GPCG15 trial 1	GPCG15 trial 2
Disc speed (rpm)	440	440
Air gap pressure (kPa)	2	2
Air flow rate (m^3/h)	148.7	148.7
Binder flow rate (g/min)	60	70
Atomization pressure (kPa)	151.7	151.7

in order to operate for less than 3 h. Also, a bed mass of 10 kg was used to approach the industrial needs instead of the 3.3 kg corresponding to the geometric scale-up value. Air gap pressure and atomization pressure were the same as the optimized set of conditions for the small-scale equipment.

With placebo 1, Froude disc velocity and air flow rate scale-up relationships without the correction factor, as given by Eqs. (1)–(7), were used to calculate the process parameters at large-scale. The product obtained contains numerous flaky agglomerates and, except for the large granules, is very dry. It suggests that, for the disc velocity used, the binder was not distributed uniformly throughout the fluid bed. The high air flow rate value used can explain also the relative dryness of the bed granules. For placebo 2, the disc peripheral velocity was set to that for the GPCG1 optimal run and the air flow rate was obtained from Eq. (7). In this case, the product properties are closer to those obtained in the small-scale unit. There are no flaky or wet agglomerates.

Acetaminophen rotogranulation trial 1 was processed with the same process parameters as for placebo 2. To evaluate the product property variations as a function of the bed moisture content, trial 2 was carried out with a binder flow rate of 70 g/min instead of 60 g/min (see Table 10). Fig. 5 shows that trials 1 and 2 both reached an equilibrium state, which is expected in a stable process. The outlet temperature of trial 2 reaches the equilibrium state more rapidly than trial 1 owing to the larger binder flow rate.

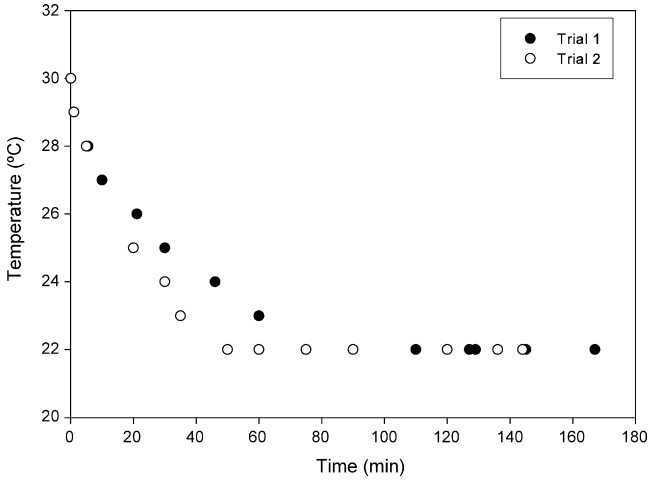

Fig. 5. Temperature evolution for the GPCG15 scale trials.

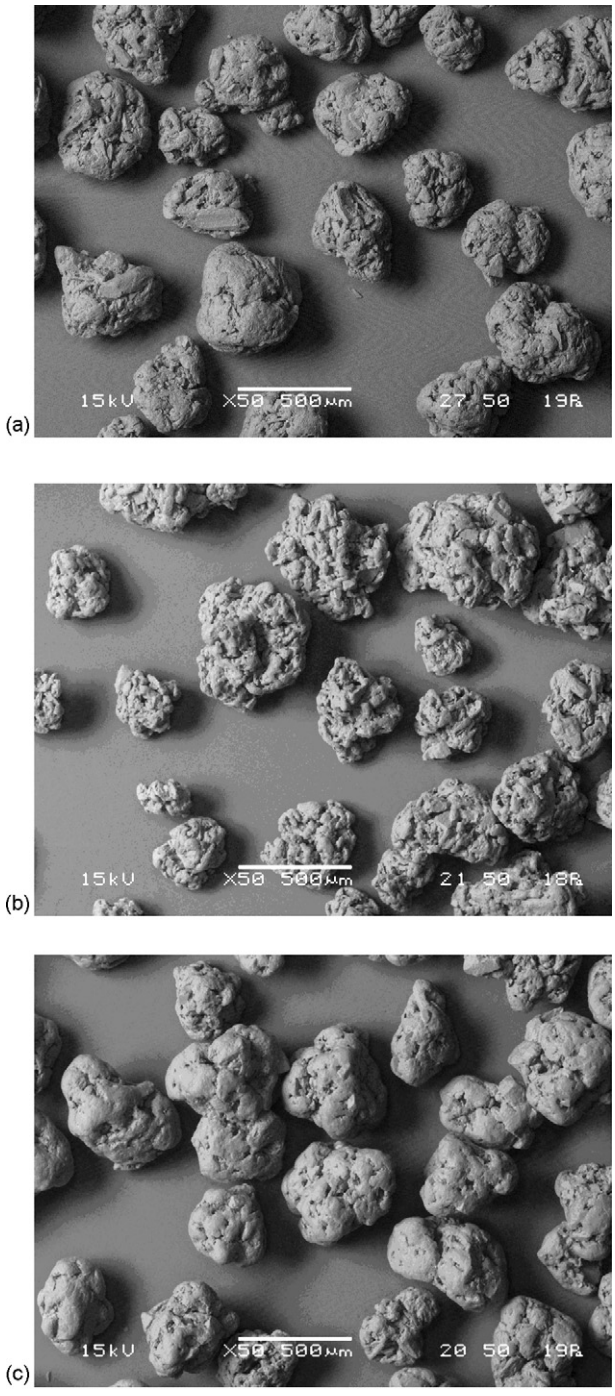

Fig. 6. SEM pictures of rotogranulation batches in GPCG1 and GPCG15: (a) optimal run in GPCG1, (b) trial 1 and (c) trial 2.

Table 11 compares the results for large-scale acetaminophen rotogranulations to those for the optimal run in the small-scale equipment. The properties obtained at large-scale are relatively

Table 11
Acetaminophen rotogranulation results in GPCG15

	GPCG1 optimal run	GPCG15 trial 1	GPCG15 trial 2
$\bar{\mu}$ (μm)	442	388	472
R.S.D. (%)	1.40	1.35	1.48
Carr's index (%)	17	14	14
Roundness	0.82	0.75	0.81
Drug content uniformity (%LC)	102.2 (R.S.D. = 1.5%)	96.9 (R.S.D. = 1.3%)	101.2 (R.S.D. = 0.8%)

close to those obtained during the optimal run in GPCG1. This indicates that the scale-up criteria used are appropriate for the operating range and formulation investigated with the GPCG15. The increase of binder flow rate to 70 g/min improves the mean size of pellets obtained without changing significantly the other final product properties. Fig. 6 shows also that increasing binder flow rate to 70 g/min results in a smoothed granule surface. This is an indication that large-scale process can be improved but no further optimizations were carried out at this point.

4. Conclusion

This work studied the rotogranulation final product properties with respect to five process parameters: (1) disc velocity, (2) air gap pressure, (3) air flow rate, (4) binder flow rate and (5) atomization pressure. A statistical linear regression model first allowed the determination of an optimized set of operating conditions in order to obtain a high quality final product, in a small-scale rotogranulation unit. The statistical model was experimentally validated, with observed variations between predicted and measured properties below 6%. Extrapolation of the process from a GPCG1 to a GPCG15 was next investigated by scaling up the optimized run from the GPCG1. Several criteria were presented to scale-up the disc velocity and the air flow rate to control the mixing intensity and the moisture bed content. The other process parameters were fixed to a practical value or simply remained constant during scale-up. Two different sets of criteria were proposed to evaluate the disc velocity at large-scale: (1) constant Froude number or (2) constant disc peripheral velocity. Placebo results showed that the second approach is the one that gives results closer to those obtained in the small-scale unit. The air flow rate was calculated versus an empirical relation involving a mass balance for water and a correction factor for the fluid bed volume and mass scaling. Finally, the large-scale acetaminophen rotogranulation experiments resulted in final product properties close to the ones obtained during the optimized run at small-scale.

Acknowledgements

The authors thank Merck Research Laboratories for support of our efforts and permission to present our findings. A special thanks to Mrs. Richard Desmangles and Pierre Lague and all fellow employees at Merck Frosst PR&D for their support, technical assistance and interest.

References

Ax, K., Feise, H., Salman, A., Sochon, R., Hounslow, M., 2006. Influence of liquid binder dispersion on agglomeration in an intensive mixer. Fifth World Congress on Particle Technology. AIChE Spring National Meeting, Orlando, Florida.

Chukwumezie, B., Wojcik, M., Malak, P., Adeyeye, M., 1994. Feasibility studies in spheronization and scale-up of ibuprofen microparticulates using the rotor disk fluid-bed technology. AAPS PharmSciTech 3 article 2.

Edmundson, I., 1967. Advances in Pharmaceutical Sciences, vol. 2. Academic Press, London.

Ghebre-Sellasie, I., Knoch, A., 2002. Encyclopedia of pharmaceutical technology, vol. 3, second ed. Marcel Dekker Inc., New-York.

Gu, L., Liew, C., Heng, P., 2004. Wet spheronization by rotary processing—a multistage single-pot process for producing spheroids. Drug Dev. Ind. Pharm. 30, 111–123.

Holm, P., Blonde, M., Wigmore, T., 1996. Pelletization by granulation in a roto-processor rp-2. Part 1: effects of process and product variables on granule growth. Pharm. Technol. Eur. 8, 22–36.

Holm, P., Jungersen, O., Schaefer, T., Kristensen, H., 1983. Granulation in high speed mixers: part 1. Effects of process variables during kneading. Pharm. Ind. 45, 806–811.

Horsthuis, G., Laarhoven, J.V., 1993. Studies on upscaling parameters of the gral high shear granulation process. Int. J. Pharm. 92, 143–150.

Iveson, S., Litster, J., Hapgood, K., Ennis, B., 2001. Nucleation, growth and breakage phenomena in agitated wet granulation processes: a review. Powder Technol. 117, 3–39.

Korakianiti, E., Rekkas, D., Dallas, P., Choulis, N., 2000. Optimization of the pelletization process in a fluid-bed rotor granulator using experimental design. AAPS PharmSciTech 1 article 35.

Kristensen, J., Schaefer, T., Kleinebudde, P., 2000. Direct pelletization in a rotary processor controlled by torque measurements. i. influence of process variables. Pharm. Dev. Technol. 5, 247–256.

Liew, C., Wan, L., Heng, P., 2000. Role of base plate rotational speed in controlling spheroid size distribution and minimizing oversize particle formation during spheroid production by rotary processing. Drug Dev. Ind. Pharm. 26, 953–963.

Perry, R., Green, D., 1997. Perry's Chemical Engineer's Handbook, seventh ed. McGraw-Hill, New-York.

Pišek, R., Planinšek, O., Tuš, M., Sršič, S., 2000. Influence of rotational speed and surface of rotating disc on pellets produced by direct rotor pelletization. Pharmazeutische Ind. 62, 312–319.

Pišek, R., Širca, J., Svanjak, G., Srčič, S., 2001. Comparison of rotor direct pelletazation(fluid bed) and extrusuion-spheronazation method for pellet production. Pharmazeutische Ind. 63, 1202–1209.

Rashid, H., 2001. Centrifugal granulating process for preparing drug-layered pellets based on microcrystalline cellulose beads. Ph.D. Dissertation. University of Helsinki.

Rashid, H., Heinmki, J., Antikainen, O., Yliruusi, J., 1999. Effects of process variables on the size, shape, and surface characteristics of microcrystalline cellulose beads prepared in a centrifugal granulator. Drug Dev. Ind. Pharm. 25, 605–611.

Vertommen, J., Kinget, R., 1997. The influence of five selected processing and formulation variables on the particle size, particle size distribution, and fri-

ability of pellets produced in a rotary processor. Drug Dev. Ind. Pharm. 23, 39–46.

Vilhelmsem, T., Kristensen, J., Schaefer, T., 2004. Melt pelletization with polyethylene glycol in a rotary processor. Int. J. Pharm. 275, 247–256.

Wan, L., Heng, P., Liew, C., 1993. Spheronization conditions on spheroid shape and size. Int. J. Pharm. 96, 59–65.

Wan, L., Heng, P., Liew, C., 1994. The role of moisture and gap air pressures in the formation of spherical granules by rotary processing. Drug Dev. Ind. Pharm. 20, 2551–2561.

Wells, J., Aulton, M., 1988. The Science of Dosage Form Design. Churchill Livingstone Inc., New York.